SUPPLEMENTARY DATA

Ablation of Atrogin-1 impairs autophagy causing cardiomyopathy and premature death.

Tania Zaglia [*1,2], Giulia Milan [*2], Aaron Ruhs [4], Mauro Franzoso [1,2], Enrico Bertaggia [1,2], Nicola Pianca [1,2], Andrea Carpi [5], Pierluigi Carullo [6], Paola Pesce [7], David Sacerdoti [7], Cristiano Sarais [8], Daniele Catalucci [5], Marcus Krüger [4], Marco Mongillo [§ 1,2,3] and Marco Sandri [§ 1,2,3,9]

[1]Department of Biomedical Sciences, University of Padova, Viale G. Colombo 3, 35121 Padova, Italy. [2]Venetian Institute of Molecular Medicine (VIMM), Via Orus 2, 35129 Padova, Italy. [3] CNR Institute of Neuroscience, Viale G. Colombo 3, 35121 Padova, Italy. [4] Max Planck Institute for Heart and Lung Research, Ludwigstrasse 43, 61231 Bad Nauheim, Germany. [5] European Institute of Oncology (IEO), Via Adamello 16, 20139 Milano, Italy. [6]National Research Council (CNR), Institute of Genetic and Biomedical Research (IRGB) - UOS of Milan, Milan, Italy and Humanitas Clinical and Research Center, via Manzoni 113, 20089 Rozzano (Milan), Italy. [7] Department of Clinical and Experimental Medicine, University of Padova, Via Giustiniani 2, 35128 Padova, Italy. [8] Department of Cardiac, Thoracic and Vascular Sciences, University of Padova, Via Giustiniani 2, 35128 Padua, Italy. [9] Telethon Institute of Genetics and Medicine (TIGEM), via P. Castellino 111, 80131 Napoli, Italy.

* and § : equal contributors

Address correspondence to: Marco Sandri, Venetian Institute of Molecular Medicine, via Orus 2, 35129 Padova, Italy. Phone: +390497923250; Fax: +390497923xx, E-mail: marco.sandri@unipd.it;

Marco Mongillo, Venetian Institute of Molecular Medicine, via Orus 2, 35129 Padova, Italy. Phone: +390497923229; Fax: +390497923250, E-mail:marco.mongillo@unipd.it

COMPETING FINANCIAL INTEREST

The authors declare no conflicting financial interests.

Content:

Supplementary Methods

Western blotting. Myocardial protein extracts were obtained from adult and aged control and Atrogin-1 KO mice as previously described (1) and protein concentration was determined by BCA assay (Pierce, Milan, Italy). Both SDS-page with Coomassie Blue and Western blotting incubation with β-tubulin were used to ensure accurate protein titration. SDS-PAGE was performed either on 3-8% or 4–12% gradient gels (Invitrogen, Milan, Italy) loading from 30 to 60 μg protein/lane. Myocardial proteins, transferred onto PVDF (Invitrogen), were processed with primary antibodies listed in **Supplementary Table 4** either 1h at room temperature or over night at 4°C. The blots were then incubated with secondary antibodies conjugated to horseradish peroxidase (Biorad, Milan, Italy) and the reactivity was revealed by enhanced chemiluminescence (Pierce). Blots were stripped using Restore Western Blotting Stripping Reagent (Pierce) according to the manufacturer's instructions and re-probed if necessary. After performing WB with the antibodies used in this study, that was repeated in triplicate, blots were re-probed with beta-tubulin when applicable as loading control.

Quantitative RT-PCR. Total RNA was prepared using the SV Total RNA Isolation System (Promega Milan, Italy) according to the manufacturer's protocol and single-strand cDNA was synthesized by SuperScript III (Invitrogen). RT-qPCR was performed using a GeneAmp 9600 thermocycler, coupled with a GeneAmp 5700 Sequence Detection System (Applied Biosystems, Monza, Italy), according to the

manufacturer's instructions, with the SYBR Green I kit (QIAGEN, Milan, Italy). The relative quantification method, described by Pfaffl (2), was used to evaluate the differences in gene expression. Values in the experiments were normalized to the expression of the GAPDH internal reference, whose abundance did not change under the experimental conditions used in the study. Gene-specific primer pairs were selected with Primer 3 software (http://frodo.wi.mit.edu/cgi-bin/primer3/primer3_www.cgi); sequences of distinct exons were chosen to avoid amplifying contaminant genomic DNA. The primer sequences used in this study are listed in **Supplementary Table 5**. The results of RTqPCR are given in arbitrary units and expressed as fold changes in mRNA levels relative to controls.

Mass spectrometry (MS)-based proteomics. Mass spectrometry (MS)-based proteomics was performed in nin mo. old control and Atrogin-1 KO hearts. Following protein extraction from the heart tissue (buffer: 4% SDS, 100mM Tris/HCl pH 7.6, 0.1M DTT) samples were separated on NuPAGE 4-12 % BIS-TRIS gel (Invitrogen, Carlsbad, USA). Gels were stained with colloidal Protein Staining Solution (Invitrogen), and 12 evenly sized gel pieces were excised and processed for mass spectrometry. The gel pieces were subjected to in gel reduction and alkylation, followed by LysC digestion as described previously (3, 4). Briefly, gel pieces were washed twice with 50 % (50 mM NH_4HCO_3 / 50 % ethanol) for 20 min and dehydrated with 100 % ethanol for 10 min and then vacuum centrifuged. Gel pieces were reduced with 10 mM DTT for 45 min at 56 °C and alkylated with 55 mM iodoacetamide (BioUltra-Sigma-Aldrich Corp.) for 30 min at RT in the dark. After two steps of washing / dehydration, samples were dehydrated twice with 100 % ethanol for 15 min and vacuum centrifuged. Gel pieces were digested overnight at 37 °C in 50 µL of digestion buffer containing 12.5 ng/µL of LysC (Wako). Released peptides were extracted (collecting separately the liquid mixture of each samples at each step) once by adding 100 µL of 30 % acetonitrile LC/MS grade (Thermo Scientific) / 3 % trifluoracetic acid (TFA, protein sequence analysis grade, Sigma-Aldrich) in water (LC/MS grade quality, Thermo Scientific), twice by adding 70 % acetonitrile, followed by two final extractions with

100 % acetonitrile. Extracts were vacuum centrifuged to remove acetonitrile and subsequently acidified with 0.5 % TFA. Samples containing peptides were desalted and concentrated with homemade "STAGE" tips (Stop and Go extraction tips) filled with C-18 (C18 Empore Disks, 3M, Minneapolis, MN) as described earlier (4, 5). Reverse phase nano-LC-MS/MS was done by using a nanoflow liquid chromatography (LC) system (Proxeon, Denmark). The LC system was coupled to LTQ-Orbitrap Velos instrument (Thermo Fisher Scientific) equipped with a nanoeletrospray source (Proxeon). Chromatographic separation of peptides was performed in a 10-cm long and 75-µm inner diameter capillary needle. The column was custom-made with methanol slurry of reverse-phase ReproSil-Pur C18-AQ 3-µm resin (Dr. Maisch GmbH). The tryptic peptide mixtures were autosampled at a flowrate of 0.5 µl/min and then eluted with a linear gradient within 150 min at a flow rate 0.25 µl/min. The LTQ-Orbitrap Velos mass spectrometer was operated in the data-dependent mode to automatically measure MS and MS/MS spectra. For CID-MS/MS top15 method, full scan MS spectra (from *m*/*z* 300–1700) were acquired in the Orbitrap analyzer after accumulation to a target value of 1e6 in the linear ion trap. Resolution in the Orbitrap system was set to r = 60,000 and the 15 most intense peptide ions with charge states ≥2 were isolated to a target value of 5,000 and fragmented in the linear ion trap CID with normalized collision energy of 35% (6). An activation q = 0.25 and activation time of 10 ms were used. For data analysis we used the MaxQuant software tool (Version 1.2.0.18). The measured raw data were processed and quantitated as described by Cox et al (7). Briefly, a peak list was generated using the following parameters: maximum mass deviation for precursor ions was 20 ppm and 0.5 Da for CID fragment ions. A maximum of 1 missed cleavage was allowed and enzyme specificity was set to LysC. In addition, the heavy amino acid Lysin-6 was chosen as fixed modification and variable modifications included Oxidation (M), and Acetyl (Protein N-term). The MaxQuant generated peak list was searched against the human International Protein Index (IPI) database v3.68 including a list of common contaminants such as keratins and concatenated with reverse copies of all

sequences. Incorporation of protein groups was calculated as relative isotope incorporation (RII) (ratio / (1 + ratio)). Following quantile normalization RII-ratios were calculated between conditions and t-tests (two sided, equal variance) were performed on duplicates from KO and WT. To perform lable-free quantification the corresponding heavy and light protein group intensities per condition were added and normalized by peptide count. Following quantile normalization protein group intensity ratios were calculated between conditions and t-tests (two-sided, equal variance) were carried out on duplicates from KO and WT.

Exercise tolerance test. Exercise tolerance test was performed using a protocol similar to that used before (8, 9). Briefly aged Atrogin-1 KO male mice and age- and sex-matched littermate controls were left to adapt to treadmill at a speed of 10 cm/sec for 5 minutes, then mice ran at a speed of 15 cm/sec for 5 minutes. Finally the speed was increased of 3cm/sec every 10 minutes until the mice were exhausted (8, 10). The exercise test was repeated another time after 24 hours.

Skeletal muscle electroporation. Adult control C57BL/6J mice underwent skeletal muscle electroporation following the procedure previously described (11).

Rat neonatal cardiomyocyte isolation and culture. P1 neonatal rats were sacrificed by cervical dislocation, hearts were removed, minced in ADS (5 mM glucose, 106 NaCl, 5.3 KCl, 20 Hepes, 0.8 Na_2HPO_4, 0.4 $MgSO_4$, in mM) and then enzimatically dissociated with collagenase A (0.4 mg/ml) (Roche) and pancreatine (1.2 mg/ml) (Sigma). Cells were cultured in medium containing 65% DMEM, 17% M199, 5% HS, 2.5% NCS, L-glutamine and antibiotics and plated on laminin-coated dishes (10 $\mu g/cm^2$) at a density of 60000 cells/cm^2 and maintained in a humidified atmosphere (5% CO_2) at 37°C.

Cell transfection. Three days after plating cardiomyocytes were transfected with the folloing vectors: i) LC3-YFP, ii) CHMP2B or iii) LC3-YFP + CHMP2B, by using transfectin (Biorad, Milan, Italy) as recommended by the manufacturer. A group of transfected cells were also treated with the 200nM Bafilomycin for 12 hours before fixation. Cells were fixed with 4% PFA 30 min. at 4°C and used for

immunofluorescence and morphometric analyses. The plasmid encoding CHMP2B was a kind gift by P.I. Hanson and M. Salvi (Dep of Biomedical Sciences, University of Padova, Italy) and LC3-YFP was kindly shared by E Kominami (Department of Biochemistry, Juntendo University School of Medicine, 2-1-1 Hongo, Bunkyo-ku, Tokyo 113-8421, Japan).

Supplementary Figure Legends

Figure 1. Atrogin-1 knock-out (KO) mice develop interstitial fibrosis and show reduced lifespan.

(**a-b**) Confocal immunofluorescence analysis on ventricular cryosections from control (**a**) and Atrogin-1 KO (**b**) mice co-stained with antibodies to sarcomeric actinin (α-actinin, green signal) and collagen I (red signal). White arrows show abundant collagen I interstitial accumulation. LA: left atrium. Scale bar: 500μm; high magnification 50μm. (**c**) Confocal immunofluorescence analysis on ventricular cryosections from control (left panel) and Atrogin-1 KO (right panel) mice stained with an antibody specific for collagen VI. Scale bar: 50μm; instets, 25μm. (**d**) Western blotting analysis on ventricular extracts from aged control (C) and Atrogin-1 KO (KO) mice, showing a significant collagen VI accumulation in Atrogin-1 KO hearts. Coomassie blue staining is shown as loading control. MW, Molecular Weight. (**e**) Exercise tolerance test in sixteen month old control (white bar) and Atrogin-1 KO (black bar) mice. Bars represent mean±s.e.m. (*, $P<0.05$; n=5 mice for each group). Note that Atrogin-1 KO mice have a reduced tolerance to exercise, compared to controls.

Figure 2. Atrogin-1 knock-out hearts show increased cardiomyocyte apoptosis and anomalous cardiomyocyte ultrastructure.

(**a**) Confocal immunofluorescence analysis on ventricular cryosections from nine month old control (left panel) and Atrogin1 KO (right panel) mice co-stained with an antibody specific for cleaved caspase-3 (red signal) and wheat germ agglutinin (wga, green signal). Arrows indicate apoptotic cardiomyocytes in an Atrogin-1 KO heart. Scale bar: 25μm. (**b**) Electron micrographs on ventricular thin sections from a sixteen mo. old Atrogin-1 KO mouse. The inset shows abnormal ER cisternae in Atrogin-1 KO cardiomyocytes. Scale bar: (left panel) 1μm; (right panel) 500 nm.

Figure 3. Atrogin-1 knock-out hearts show impaired autophagy.

(**a**) Confocal immunofluorescence analysis on ventricular cryosections from sixteen month old Atrogin-1 KO mice co-stained with antibodies specific for sarcomeric actinin (α-actinin, green signal) and LC3 (red signal), showing LC3 accumulation in Atrogin-1 KO cardiomyocytes (white arrows). Images are details from the LV. Scale bars: 25μm. (**b**) Confocal immunofluorescence analysis on ventricular cryosections from sixteen month old Atrogin-1 KO mice co-stained with antibodies against LC3 (green signal) and p62 (red signal), showing no co-expression of LC3 and p62 aggregates in Atrogin-1 KO LV cardiomyocytes. Scale bar: 25μm. (**c-d**) Confocal immunofluorescence analysis on ventricular cryosections from wild-type mice (**c**) and wild-type mice which undergone nutrient deprivation (**d**), co-stained with antibodies against LC3 (green signal) and p62 (red signal). Scale bar: 25μm.

Figure 4. No LC3 and LAMP2 co-expression in aged Atrogin-1 knock-out cardiomyocytes.

(**a**) Confocal immunofluorescence analysis on ventricular cryosections from sixteen month old Atrogin-1 KO mice co-stained with antibodies against LC3 (green signal) and LAMP2 (red signal), showing no co-expression of LC3 and LAMP2 in Atrogin-1 KO cardiomyocytes. Images are details from the LV. The merge image of LC3, LAMP2 and bright field is shown. Scale bars: (**a**) 25μm; inset, 5μm. (**b-d**) Confocal

immunofluorescence analysis on ventricular cryosections from wild-type mice (**b**) and wild-type mice which undergone nutrient deprivation (**c**) or bafilomycin treatment (**d**) and co-stained with antibodies specific for LC3 (green signal) and p62 (red signal). Scale bar: 20μm; insets 5μm.

Figure 5. CHMP2B accumulation in Atrogin-1 knock-out cardiomyocytes.

(**a-b**) Confocal immunofluorescence analysis on ventricular cryosections from sixteen month old control (**a**) and Atrogin-1 KO (**b**) mice co-stained with antibodies against sarcomeric actinin (α-actinin, green signal) and CHMP2B (red signal), showing accumulation of CHMP2B in Atrogin-1 KO cardiomyocytes (white arrows). Images are details from the LV. Scale bars: 50μm; (inset) 10 μm. (**c**) Confocal immunofluorescence analysis of ventricular cryosections from sixteen month old Atrogin-1 KO mice co-stained with antibodies against CHMP2B (green signal) and LAMP2 (red signal), showing no co-expression of LAMP2 and CHMP2B in Atrogin-1 KO cardiomyocytes. Scale bar: 25μm; inset 7μm.

Figure 6. CHMP2B accumulation in cultured cardiomyocytes upon MG132 cell treatment.

(**a-b**) Confocal immunofluorescence analysis on control (**a**) and MG132-treated (**b**) neonatal cultured cardiomyocytes co-stained with antibodies against cardiac Troponin I (cTnI, green signal) and CHMP2B (red signal), showing CHMP2B accumulation in MG132-treated cells. Note that CHMP2B accumulates in cardiomyocyte areas characterized by sarcomeric depletion. Nuclei were counterstained with DAPI (blue signal). Scale bars: 25μm; insets in (**a**) 10μm and 1μm; insets in (**b**) 10μm and 5μm.

Figure 7. Adenoviral mediated CHMP2B down-regulation in Atrogin-1 knock-out mice.

(**a**) Confocal immunofluorescence analysis on ventricular cryosections from Atrogin-1 KO mice injected with an AAV9-GFP-U6-CHMP2Bsh viral vector co-stained with antibodies specific for GFP (**a**, green

signal, left panel) and CHMP2B (red signal, middle panel). The right panel represents the merge of (**t**he left) and (the middle) panels. Note that CHMP2B signal is significantly lower in GFP positive cardiomyocytes indicating the efficiency of CHMP2B down-regulation. Scale bar: 25µm. (**b**) Confocal immunofluorescence analysis on ventricular cryosections from Atrogin-1 KO mice injected with an AAV9-GFP control viral vector co-stained with antibodies specific for GFP (green signal, left panel) and CHMP2B (red signal, middle panel). The right panel represents the merge of (the left) and (the middle) panels. Note no decrease in CHMP2B signal in GFP positive cardiomyocytes. Scale bar: 25µm.

Supplementary References.

1. Sandri, M., Sandri, C., Gilbert, A., Skurk, C., Calabria, E., Picard, A., Walsh, K., Schiaffino, S., Lecker, S.H., and Goldberg, A.L. 2004. Foxo transcription factors induce the atrophy-related ubiquitin ligase atrogin-1 and cause skeletal muscle atrophy. *Cell* 117:399-412.
2. Pfaffl, M.W. 2001. A new mathematical model for relative quantification in real-time RT-PCR. *Nucleic Acids Res* 29:e45.
3. Shevchenko, A., Tomas, H., Havlis, J., Olsen, J.V., and Mann, M. 2006. In-gel digestion for mass spectrometric characterization of proteins and proteomes. *Nat Protoc* 1:2856-2860.
4. Kruger, M., Moser, M., Ussar, S., Thievessen, I., Luber, C.A., Forner, F., Schmidt, S., Zanivan, S., Fassler, R., and Mann, M. 2008. SILAC mouse for quantitative proteomics uncovers kindlin-3 as an essential factor for red blood cell function. *Cell* 134:353-364.
5. Rappsilber, J., Ishihama, Y., and Mann, M. 2003. Stop and go extraction tips for matrix-assisted laser desorption/ionization, nanoelectrospray, and LC/MS sample pretreatment in proteomics. *Anal Chem* 75:663-670.
6. Olsen, J.V., Macek, B., Lange, O., Makarov, A., Horning, S., and Mann, M. 2007. Higher-energy C-trap dissociation for peptide modification analysis. *Nat Methods* 4:709-712.
7. Cox, J., Matic, I., Hilger, M., Nagaraj, N., Selbach, M., Olsen, J.V., and Mann, M. 2009. A practical guide to the MaxQuant computational platform for SILAC-based quantitative proteomics. *Nat Protoc* 4:698-705.
8. He, C., Bassik, M.C., Moresi, V., Sun, K., Wei, Y., Zou, Z., An, Z., Loh, J., Fisher, J., Sun, Q., et al. 2012. Exercise-induced BCL2-regulated autophagy is required for muscle glucose homeostasis. *Nature* 481:511-515.
9. Grumati, P., Coletto, L., Schiavinato, A., Castagnaro, S., Bertaggia, E., Sandri, M., and Bonaldo, P. 2011. Physical exercise stimulates autophagy in normal skeletal muscles but is detrimental for collagen VI-deficient muscles. *Autophagy* 7:1415-1423.
10. Wende, A.R., Schaeffer, P.J., Parker, G.J., Zechner, C., Han, D.H., Chen, M.M., Hancock, C.R., Lehman, J.J., Huss, J.M., McClain, D.A., et al. 2007. A role for the transcriptional coactivator PGC-1alpha in muscle refueling. *J Biol Chem* 282:36642-36651.

11. Sandri, M., Bortoloso, E., Nori, A., and Volpe, P. 2003. Electrotransfer in differentiated myotubes: a novel, efficient procedure for functional gene transfer. *Exp Cell Res* 286:87-95.

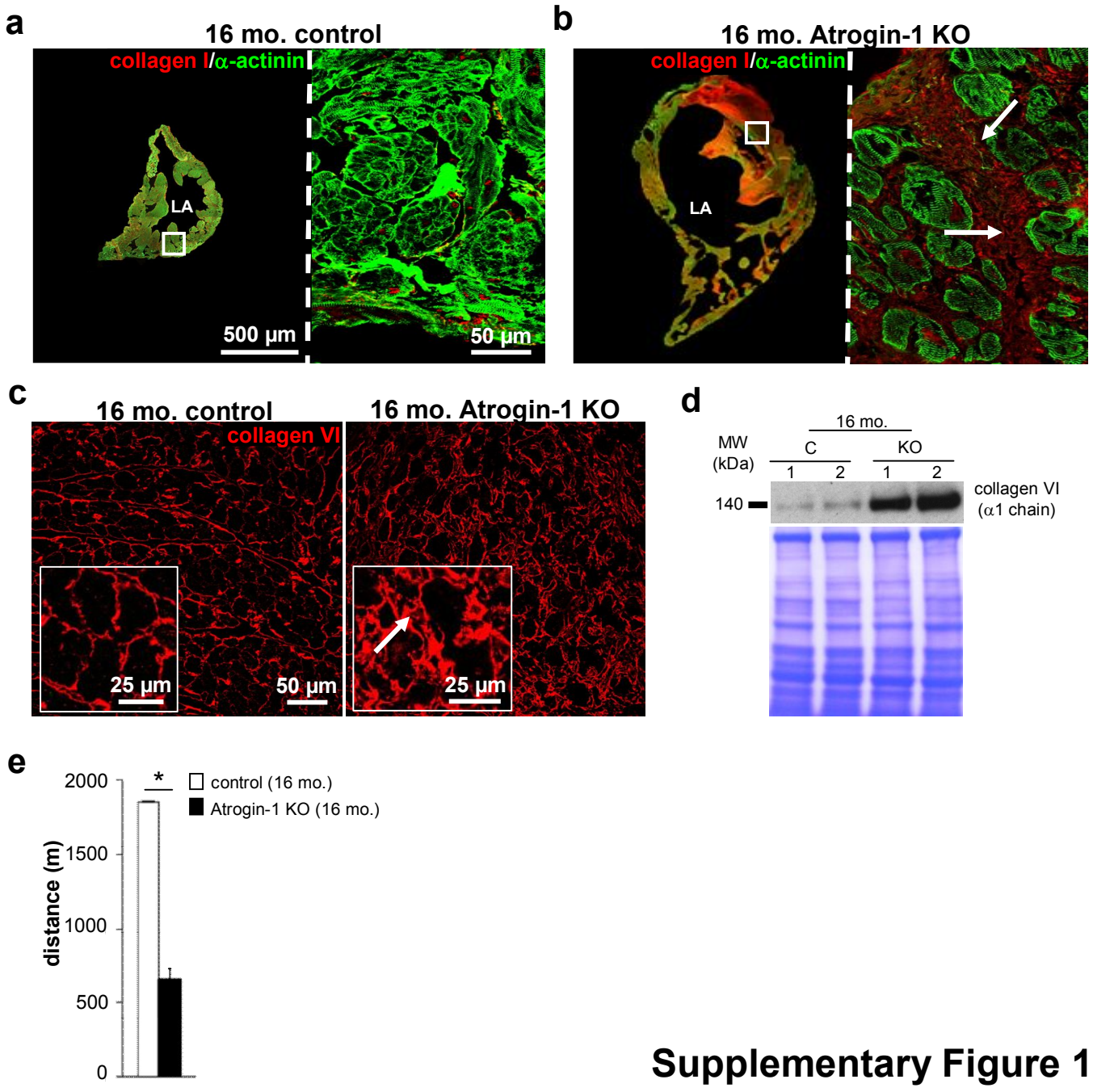

Supplementary Figure 1

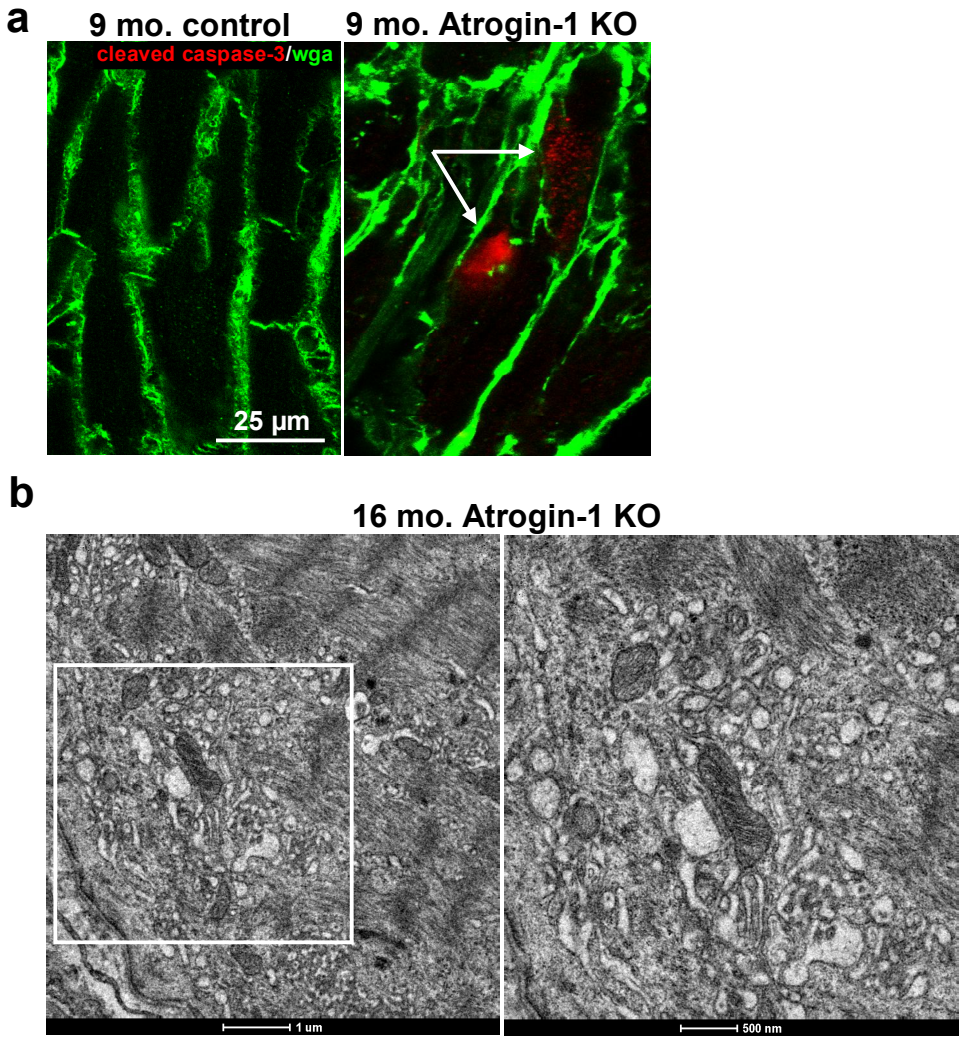

Supplementary Figure 2

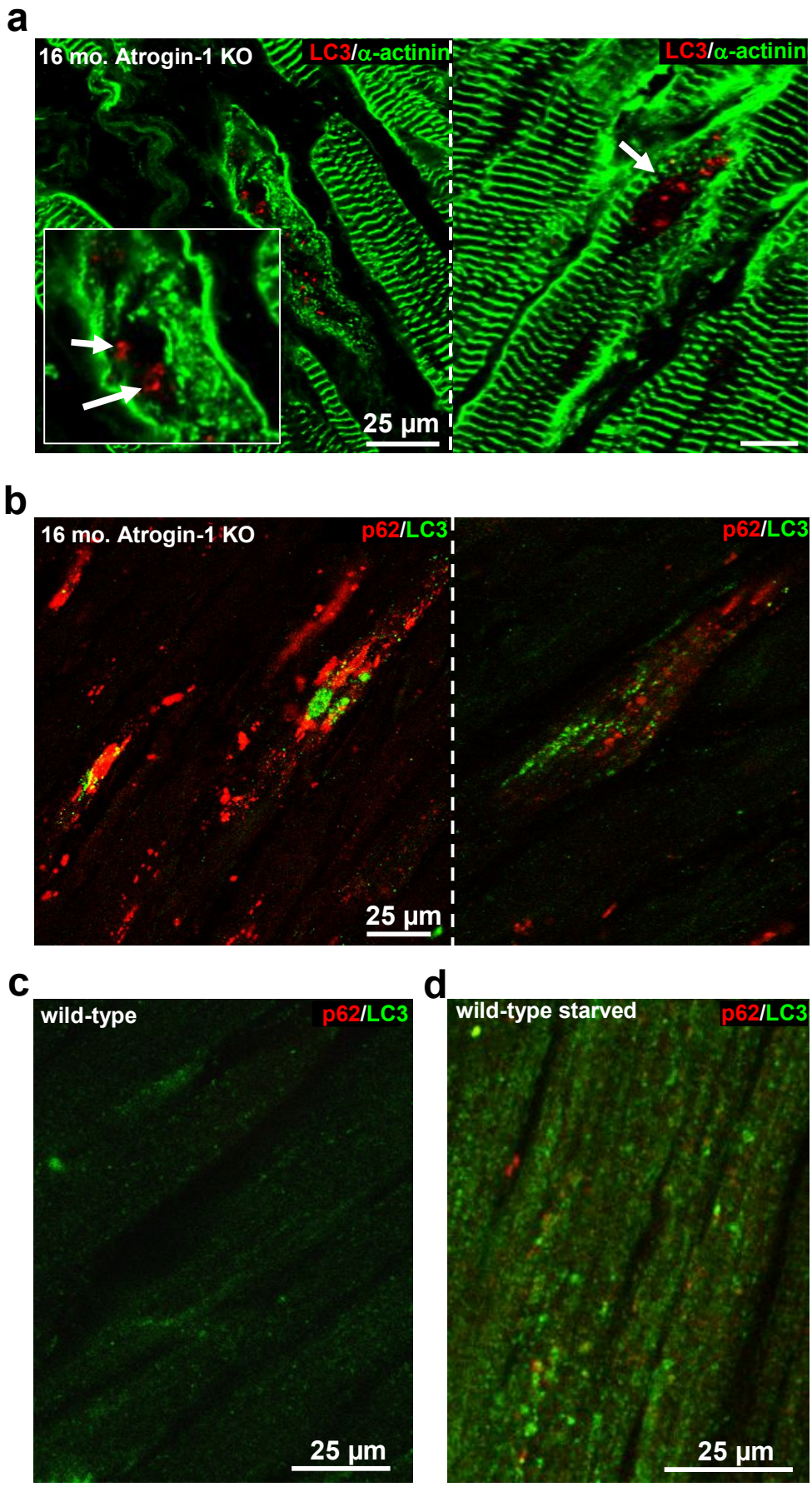

Supplementary Figure 3

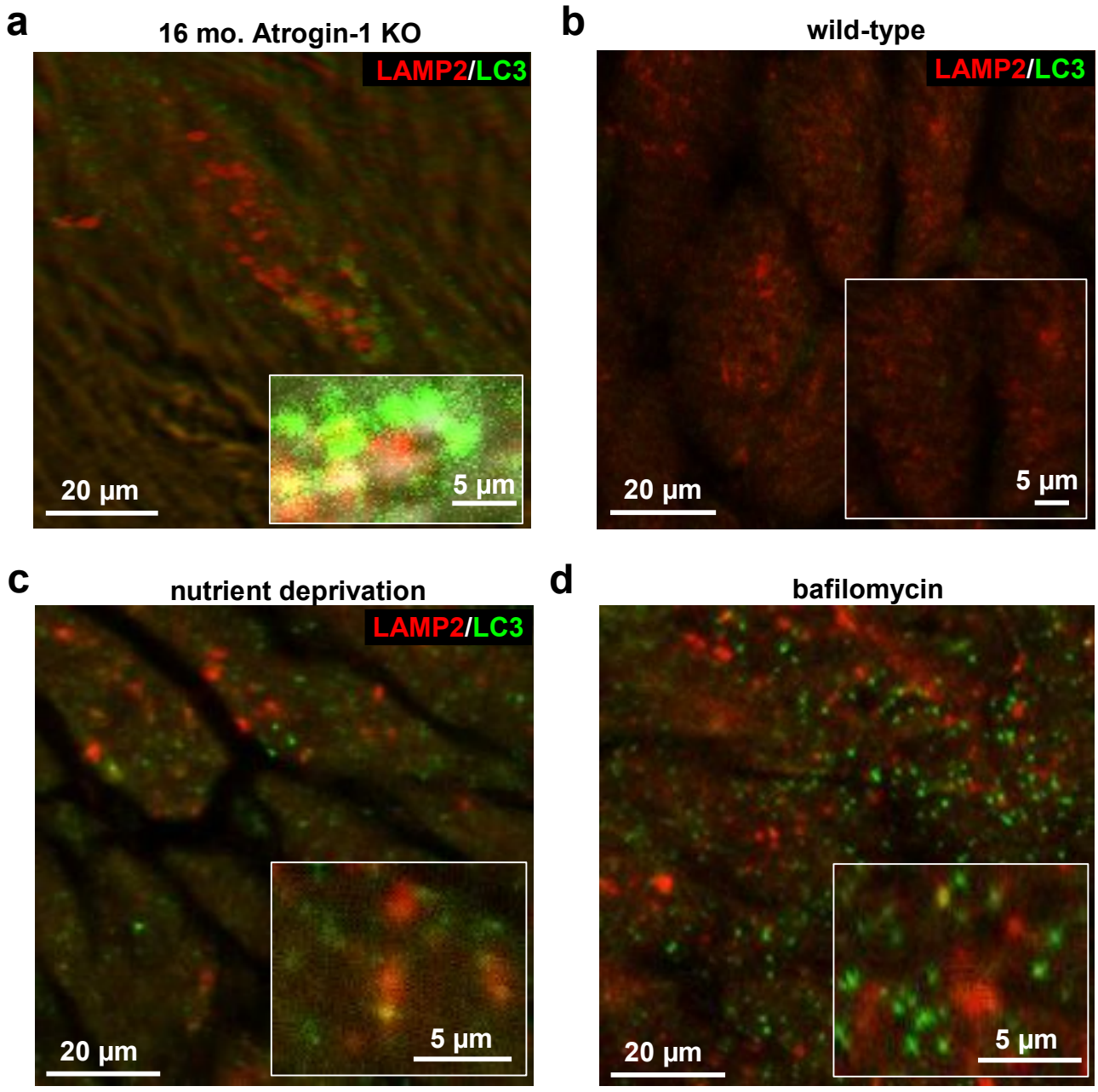

Supplementary Figure 4

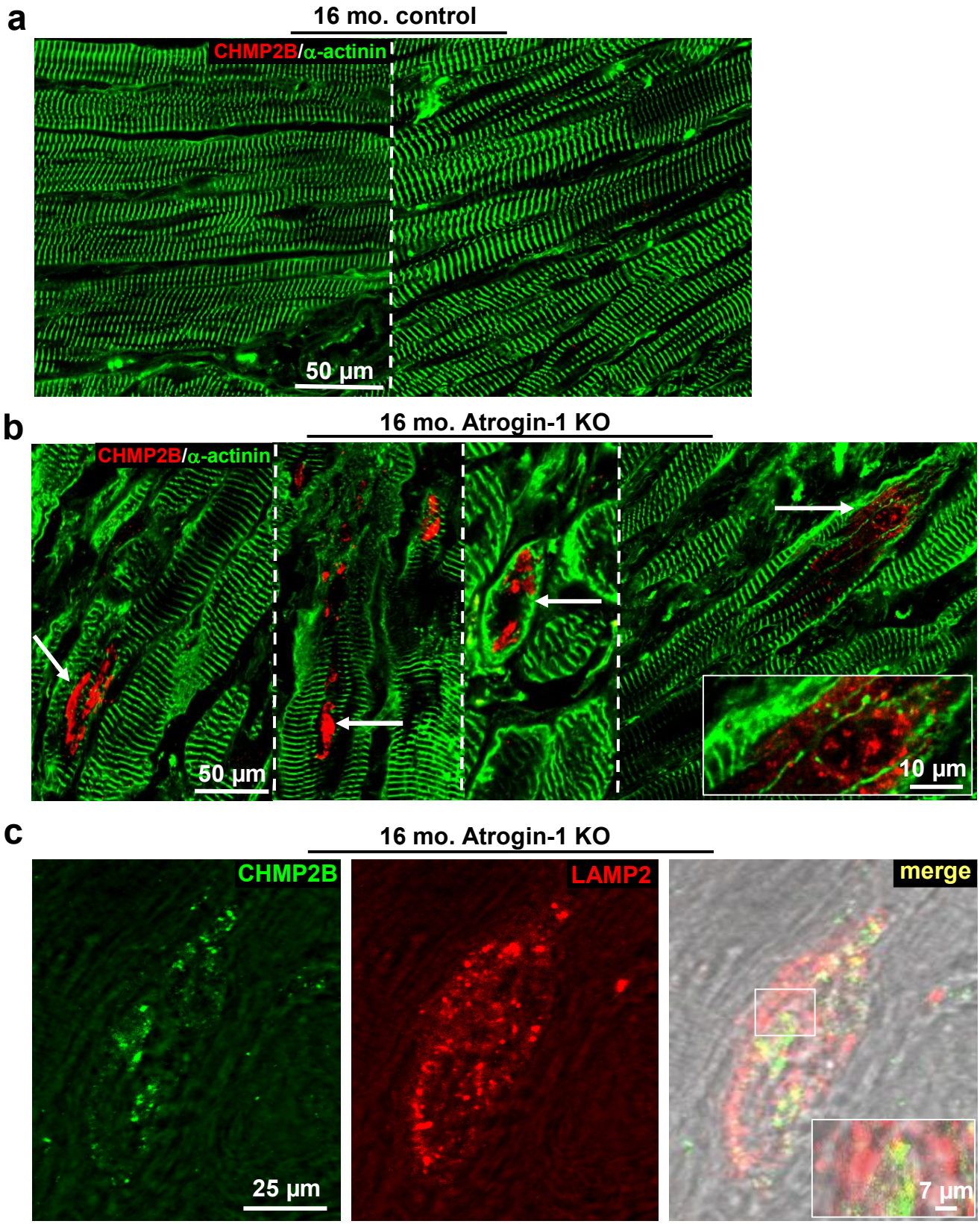

Supplementary Figure 5

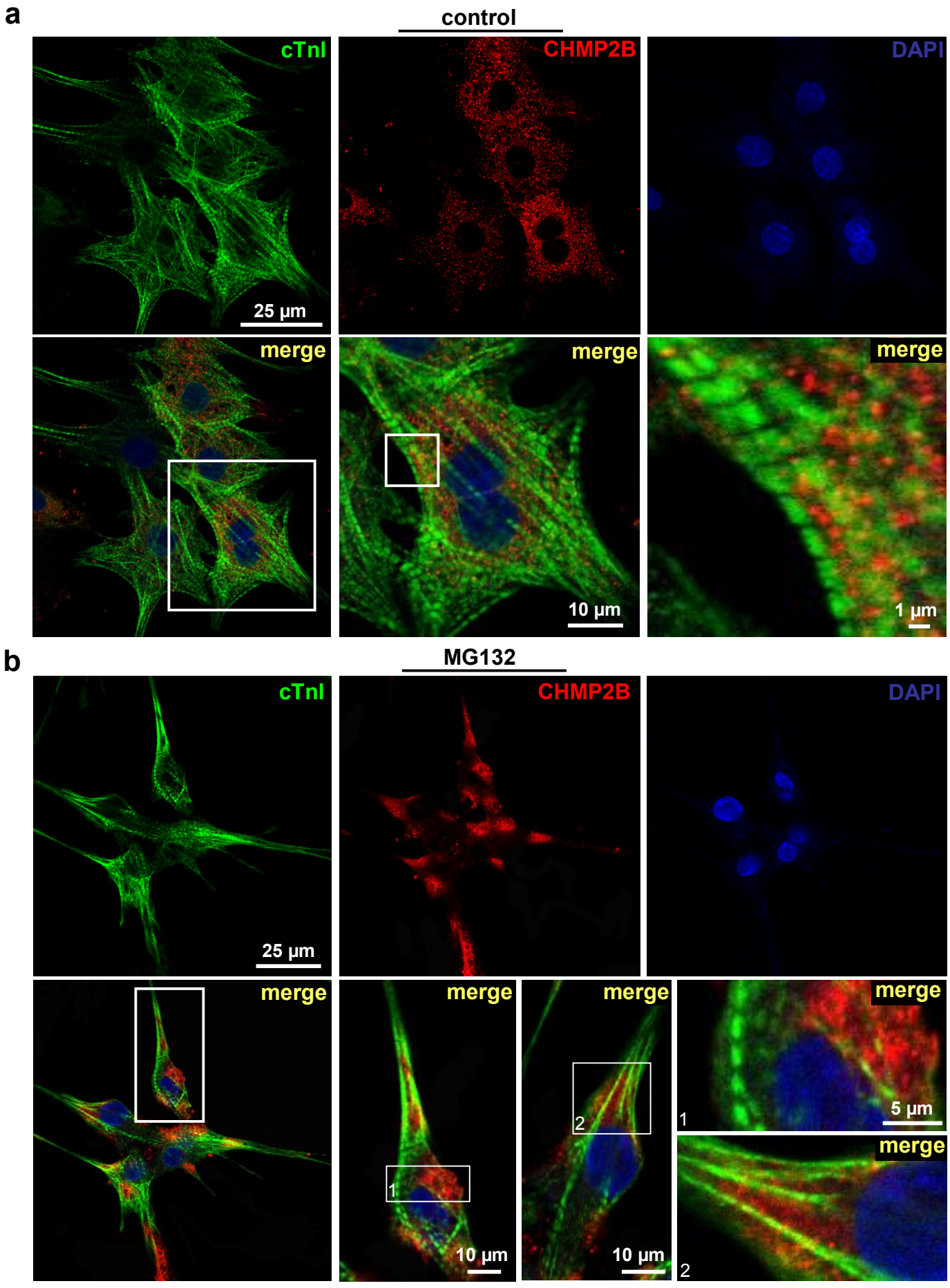

Supplementary Figure 6

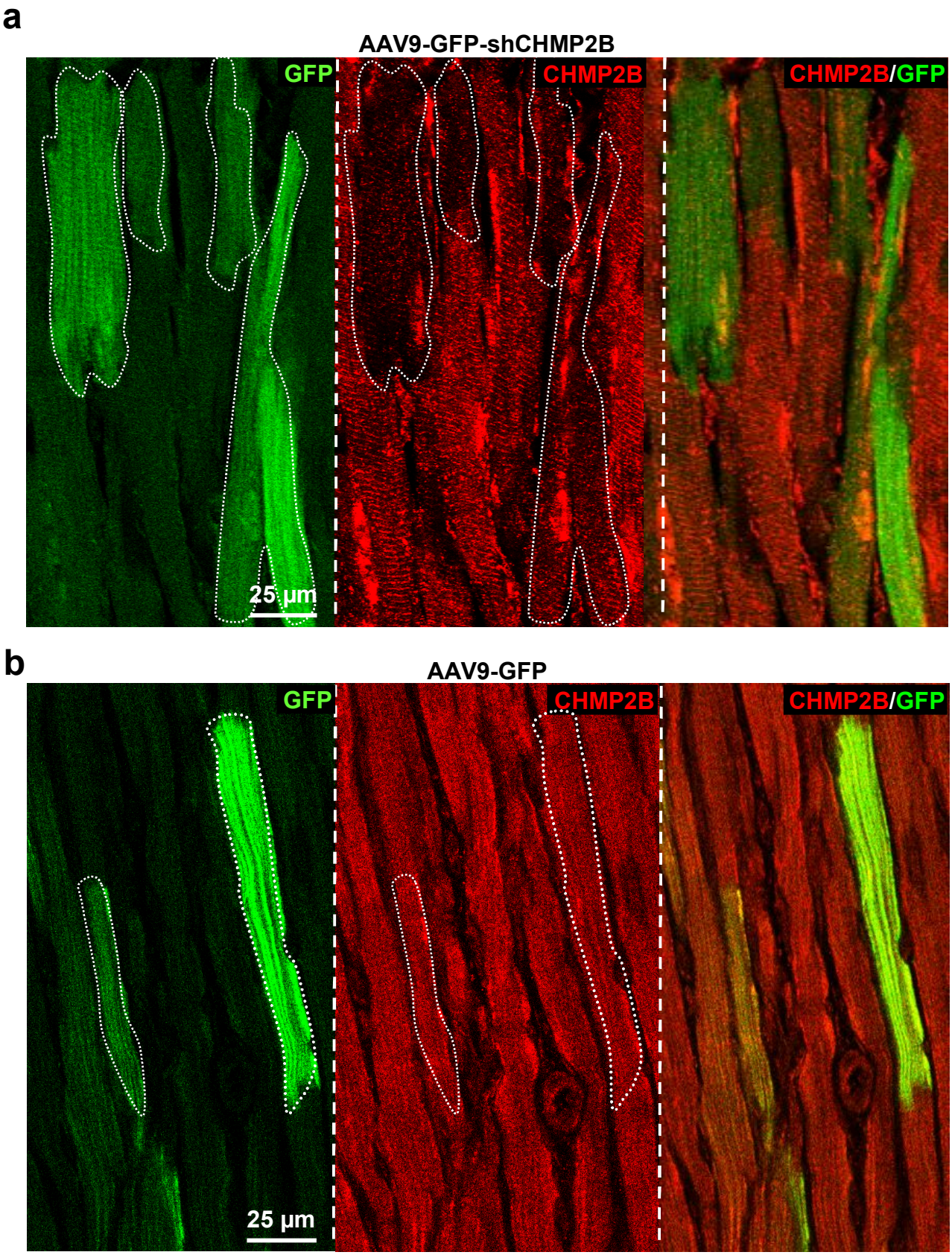

Supplementary Figure 7

Parameters	Controls (n=5)	MAFbx KO (n=7)	P-value
LV mass (mg)	106.5±15.3	133±31	<0.05
AAPD (mm)	2.1±0.3	4.3±0.4	<0.01
Sphericity Index (d.)	0.45±0.1	0.81±0.1	<0.01
Sphericity Index (s.)	0.34±0.1	0.57±0.1	<0.05

Supplementary Table 1. Ecocardiography analysis in 16 month old control and Atrogin-1 KO mice. Abbreviations: LV: Left Ventricle; AAPD: Atrium Antero-Posterior Diameter; d.: diastole; s.: systole; n.s.: no significant.

Protein Names	Gene Names	T test
Ras-related protein Rab-2A	Rab2a	0,0258
Myo18b protein	Myo18b	0,0458
UPF0568 protein C14orf166 homolog	2700060E02Rik	0,0003
Beta-coat protein	Copb1	0,0108
Calcium/calmodulin-dependent protein kinase type II subunit delta	Camk2d	0,0290
6-phosphofructokinase, muscle type	Pfka	0,0051
Programmed cell death 6 interacting protein	Pdcd6ip	0,0208
15S Mg(2+)-ATPase p97 subunit	Vcp	0,0344
BCL2-associated athanogene 3	Bag3	0,0361
Adenylate kinase 3-like	Ak3b	0,0061
Diadenosine tetraphosphate synthetase	Gars	0,0284
Ankyrin repeat domain-containing protein 25	Ankrd25	0,0228
T-complex protein 1 subunit beta	Cct2	0,0373
Dynamin UDNM	Dnm2	0,0456
Ubiquitin-activating enzyme E1	Sbx	0,0035
Putative uncharacterized protein	Clip1	0,0104
LAMP-1	Lamp1	0,0144
Molecule associated with JAK3 N-terminus	Myo18a	0,0331
Eukaryotic translation initiation factor 4 gamma 1	Eif4g1	0,0177
Endoplasmic reticulum resident protein 72	Cai	0,0469
MKIAA0899 protein	Ap2a2	0,0248
Beta-taxilin	Mdp77;Txlnb	0,0410
Cytidine monophosphate kinase	Cmk	0,0119
Elongin 15 kDa subunit	Tceb1	0,0263
Microtubule-associated protein tau	Mapt	0,0185
Anxa6 protein	Anxa6	0,0026
14-3-3 protein gamma	Ywhag; 14-3-3 gamma	0,0025
Metaxin-2	MNCb-0780	0,0206
Sorbs2 protein	Sorbs2;Argbp2; Kiaa0777	0,0004
5-aminoimidazole-4-carboxamide ribonucleotide formyltransferase	Atic;Purh	0,0412
Probable C->U-editing enzyme APOBEC-2	Apobec2	0,0273
Macrophage 23 kDa stress protein	Msp23	0,0166
Alpha-glucosidase 2	G2an	0,0059
BPG-dependent PGAM 2	Pgam2	0,0141
Protein disulfide-isomerase A6	Pdia6;Txndc7	0,0157
Fructose-bisphosphate aldolase	Aldoa	0,0185
Importin alpha-S2	Kpna	0,0336
ATP-binding cassette sub-family F member 2	Abcf2	0,0245
MACRO domain-containing protein 1	Lrp16;Macrod1	0,0139
Nicotinamide phosphoribosyltransferase	Nampt	0,0349
NEDD8 carrier protein	Ubc12	0,0476
Guanosine diphosphate dissociation inhibitor 1	Gdi1	0,0251
BPG-dependent PGAM 1	Pgam1	0,0000
Ras-related protein Rab-6A	MNCb-1660;Rab6	0,0234
Nuclear protein localization protein 4 homolog	Kiaa1499	0,0220
C-1-tetrahydrofolate synthase, cytoplasmic	Mthfd1;Dcs	0,0468
DEAD (Asp-Glu-Ala-Asp) box polypeptide 19b	Ddx19b	0,0342
Adipocyte protein S3-12	Kiaa1881	0,0008
B-CAM cell surface glycoprotein	Bcam	0,0454
Iron-sulfur cluster assembly enzyme ISCU, mitochondrial	Iscu;Nifun	0,0095

Cardiovascular heat shock protein;Heat shock protein 25 kDa 2	Cvhsp	0,0339
78 kDa glucose-regulated protein;Heat shock 70 kDa protein 5	Grp78	0,0335
F-actin-capping protein subunit beta	Cappb1	0,0063
Calcium-transporting ATPase sarcoplasmic reticulum type	Atp2a2	0,0287
Importin subunit alpha-4	Kpna4	0,0262
Hippocampal cholinergic neurostimulating peptide	Pbp	0,0423
Protein Hook homolog 3	Hook3	0,0380
Glyceraldehyde-3-phosphate dehydrogenase	Gapd	0,0293
ATP-AMP transphosphorylase 1	Ak1	0,0227
MKIAA0838 protein	Gls	0,0168
Leiomodin-2	Lmod2	0,0415
Glucose-6-phosphate isomerase	Gpi;Gpi1	0,0482
Phosphoglucomutase 2	Pgm2	0,0489
Rab3 GTPase-activating protein 150 kDa subuni	Kiaa0839	0,0306
Dystrophin	Dmd	0,0421
ADP-ribosylation factor 1	Arf1	0,0159
ER-Golgi intermediate compartment 53 kDa protein	Ergic53;Lman1	0,0222
28S ribosomal protein S31, mitochondrial	Imogn38;Mrps31	0,0348
Actin-binding-like protein; Filamin C	Abpl;Fln2;Flnc	0,0041
Aldehyde reductase	Akr1b1	0,0363
Protein-tyrosine phosphatase SYP	Ptpn11	0,0073
Corticosteroid-binding globulin;Serpin A6	Cbg	0,0219
Heme oxygenase 2	Hmox2	0,0209
Bendless-like ubiquitin-conjugating enzyme;Ubc13	Blu	0,0098
Obscurin	Gm878	0,0148
CapZ alpha-2	Cappa2	0,0195
Glutathione S-transferase P 1	Gstp1	0,0461
Cytoplasmic dynein 1 intermediate chain 2	Dnci2	0,0298
Cadherin 2	Cdh2	0,0390
HESB-like domain-containing protein 2	Hbld2;Isca1	0,0137
F-actin-binding protein	Nexn	0,0277
Myomesin family member 1	Myom1	0,0247
56 kDa selenium-binding protein	Lpsb	0,0087
Cysteine-rich protein 2	Crip2	0,0107
Fermitin family homolog 2	Fermt2	0,0004
[Pyruvate dehydrogenase [lipoamide]] kinase isozyme 4, mitochondrial	Pdk4	0,0239
Cardiac muscle troponin T	Tnnt2	0,0296
Ubc protein	Ubc	0,0377
Ubiquitin-fold modifier 1	Ufm1	0,0363
3-oxoacid-CoA transferase 1	Oxct	0,0420
Aldoketomutase;Glyoxalase I	Glo1	0,0414
UPF0317 protein C14orf159 homolog, mitochondrial	9030617O03Rik	0,0031
Tropomodulin 1	mCG_14153	0,0155
LDH heart subunit	Ldh2	0,0114
Phosphoglycerate kinase 1	Pgk1	0,0003
Putative uncharacterized protein	Lrrfip2	0,0033
Cysteine and glycine-rich protein 3	Clp	0,0009
Cytosolic malate dehydrogenase	Mdh1	0,0102
Actin-RPV	Actr1a	0,0035
Coiled-coil domain containing 141;MCG142258	Ccdc141	0,0086
Alcohol dehydrogenase iron-containing protein 1	Adhfe1	0,0393
Glutathione-independent PGD synthase	Ptgds	0,0113
Isochorismatase domain-containing protein 1	Isoc1	0,0242

S100 calcium binding protein A1	S100a1	0,0088
Triosephosphate isomerase	Tpi	0,0441
Complex III subunit 8	Uqcrq	0,0182
Myosin regulatory light chain 2, ventricular/cardiac muscle isoform	Myl2;	0,0256
2-phospho-D-glycerate hydro-lyase	Eno3	0,0014
Aspartate aminotransferase, cytoplasmic	Got1	0,0298
Pleckstrin homology domain containing, family C	Fermt2	0,0039
Pyruvate dehydrogenase phosphatase regulatory subunit, mitochondrial	Kiaa1990	0,0280
Mannose-6-phosphate isomerase	Mpi	0,0041
Putative uncharacterized protein	Nqo2	0,0229
Leucine zipper and CTNNBIP1 domain-containing protein	Lzic	0,0491
SH3 domain-binding glutamic acid-rich protein	Sh3bgr	0,0420
Cytochrome c oxidase subunit 7A2, mitochondrial	Cox7a2	0,0058
Four and a half LIM domains protein 2	Fhl2	0,0028
AMP deaminase 3	Ampd3	0,0349
Iron-sulfur subunit of complex II	Sdhb	0,0312
Cardiomyopathy-associated protein 1	Cmya1	0,0290
Myosin light chain 1	Mlc1v	0,0200
Troponin C	Tncc	0,0137
Actin-depolymerizing factor	Gsb	0,0042
Myosin regulatory light chain 2, atrial isoform	Myl7	0,0428
LIM domain-binding protein 3	Kiaa0613	0,0418
Collagen alpha-6(VI) chain	Col6a6	0,0420
Myosin heavy chain 2b	Myh4	0,0223
Cardiac troponin I	Tnni3	0,0180
S1 RNA-binding domain-containing protein 1	Srbd1	0,0176
Myosin light chain 1, atrial/fetal isoform	Mlc1a	0,0006
Myosin heavy chain, cardiac muscle alpha isoform	Myh6	0,0011
Sodium channel protein cardiac muscle subunit alpha	Scn5a	0,0104
Creatine kinase M chain	Ckm	0,0191
Gamma-tropomyosin	Tpm3	0,0004
Alpha-tropomyosin	Tpm1	0,0239
Actin, alpha cardiac muscle 1	Actc1	0,0036
Laminin subunit beta-2	Lamb2	0,0026

Supplementary Table 2. Protein turnover down in Atrogin-1 KO mice.

Protein Names	Gene Names	T test
Beta-actin-like protein 2	Actbl2	0,0026
PC1-like 3 protein	71B10	0,1224
Alpha-tropomyosin	Tpm1	0,0198
CCT-zeta-2	Cct6b	0,4533
Myosin heavy chain 2b	Myh4	0,0006
Cardiac troponin I	Tnni3	0,0011
Endoplasmic reticulum resident protein 29	Erp29	0,4547
ATP-binding cassette, sub-family B (MDR/TAP), member 7	Abcb7	0,3440
Acylase III	Acy3	0,0420
Cytochrome c oxidase subunit 7A1, mitochondrial	Cox7a	0,0974
Troponin C, slow skeletal and cardiac muscles	Tncc	0,1781
GCN1 general control of amino-acid synthesis 1-like 1 (Yeast)	Gcn1l1	0,0428
Phosphoglycerate kinase 1	Pgk1	0,6515
Cytochrome c oxidase subunit 7A2, mitochondrial	Cox7a2	0,0033
1,5-anhydro-D-fructose reductase	Akr1cl2	0,0349
Clathrin interactor 1	Clint1	0,0523
Mannose-6-phosphate isomerase	Mpi	0,2309
Integrin alpha-7	Itga7	0,0229
GrinchGEF	Arhgef10	0,4608
Actin-RPV	Actr1a	0,2122
CLIP-associating protein 2	Clasp2	0,0086
LIM domain-binding protein 3	Kiaa0613	0,1479
Cysteine--tRNA ligase	Cars2	0,0794
Connectin	Ttn	0,5047
Nucleoside diphosphate-linked moiety X motif 8, mitochondrial	Nudt8	0,4567
GTP-binding protein SAR1b	Sar1b	0,2162
Protein transport protein Sec61 subunit beta	Sec61b	0,3834
Biliverdin reductase A	Blvra	0,2495
Magnesium-dependent phosphatase 1	Mdp1	0,3059
Melanoma inhibitory activity protein 3	Kiaa0268	0,2035
F-actin-binding protein	Nexn	0,1319
Beta-I spectrin	Spnb1	0,3415
Myomesin family member 1	Myom1	0,0247
Acylglycerol kinase, mitochondrial	Agk	0,6381
NHL repeat-containing protein 2	Nhlrc2	0,0087
La autoantigen homolog	Ssb	0,3466
Caldesmon 1	Cald1	0,3451
1,4-alpha-glucan-branching enzyme	Gbe1	0,2482
Nebulin-related-anchoring protein	Nrap	0,5140
Dystrophin	Dmd	0,2741
Nuclear protein localization protein 4 homolog	Kiaa1499	0,2031
Amyloid beta precursor protein-binding protein 1	Appbp1	0,0159
Glyceraldehyde-3-phosphate dehydrogenase	Gapd	0,0468
2-methyl branched chain acyl-CoA dehydrogenase	Acadsb	0,1400
[Acyl-carrier-protein] malonyltransferase	Mcat	0,0227
NEDD8 carrier protein	Ubc12	0,4259
Heat shock 70 kDa protein 8	Hsc70	0,5785
Aortic preferentially expressed protein 1	Apeg1	0,5401
Alpha-soluble NSF attachment protein	Napa	0,0251
Activated protein C-binding protein	Apoh	0,1992

[Acyl-carrier-protein] S-acetyltransferase	Fasn	0,0929
Putative uncharacterized protein;MKIAA0899 protein	Ap2a2	0,0801
Glycerol-3-phosphate dehydrogenase 1-like protein	Gpd1l	0,2985
Microtubule-associated protein tau	Mapt	0,3424
Protein TBRG4	Kiaa0948	0,0248
Elongin 18 kDa subunit	Tceb2	0,2589

Supplementary Table 3. Protein concentration up in Atrogin-1 KO mice.

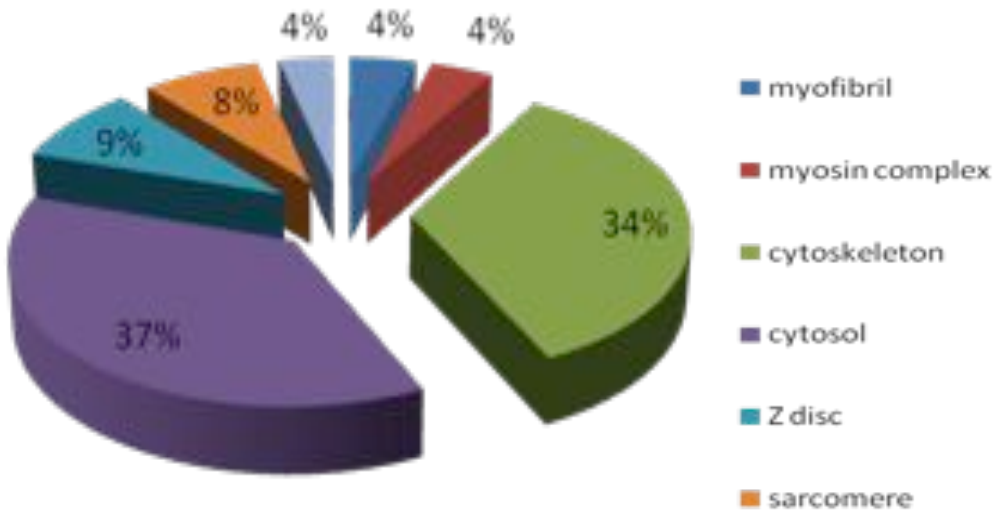

Supplementary Table 4. SILAC-based proteomics showed anomalous accumulation of proteins from different cellular compartments in adult Atrogin-1 KO hearts.

Antibody	Customer	Dilution	Analysis
mouse anti-α-actinin	Sigma	1:500	IF
rabbit anti-total Akt	Cell Signaling	1:1000	WB
rabbit anti-P-Akt (Ser473)	Cell Signaling	1:500	WB
rabbit anti-P-A.C.C	Cell Signaling	1:1000	WB
rabbit anti-Atrial Natriuretic Factor (ANF)	Peninsula Lab.	1:500	IF
rabbit anti-beclin	Santa Cruz	1:1000	WB
mouse anti-BIP	BD	1:1000	WB
rabbit anti-Bnip3	Sigma (clone Ana40)	1:3000	WB
rabbit anti-CHMP2B	Abcam	1:200/1:1000	IF/WB
rabbit anti-collagen I	Acris	1:800	IF
rabbit anti-collagen VI	Santa Cruz	1:1000	WB
rabbit anti-collagen VI	(1)	1:500	IF
rabbit anti-dystrophin	Abcam	1:600	IF
rabbit anti-anti-eiF2α	Abcam	1:1000	WB
rabbit anti-anti-P-eiF2α	Abcam	1:1000	WB
mouse anti-Flag	Sigma	1:100/1:1000	IP/WB
rabbit anti-P-Ikb	Biosurce	1:1500	WB
FITC-isolectine B4	Vector	1:200	IF
rat anti-LAMP2a	Abcam	1:500	IF
rabbit anti-LAMP2	Abcam	1:1000	WB
rabbit anti-LC3	Cell Signaling	1:200/1:1000	IF/WB
mouse anti-β-MHC	(2)	1:50/1:1000	IF/WB
rabbit anti Myc-tag	Cell Signaling	1:1000	WB
guinea pig anti-P62	New England Biolabs	1:200/1:1000	IF/WB
rabbit anti-RSK2	Cell Signaling	1:50/1:1000	IF/WB
rabbit anti-total S6	Cell Signaling	1:1000	WB
rabbit anti-P-S6	Cell Signaling	1:1000	IF
rabbit anti-skeletal actin	Abcam	1:100/1:1000	IF/WB
FITC-anti-Smooth Muscle Actin (SMA)	Sigma (clone 1A4)	1:1500	IF
rabbit anti-TAU	Accu-Specs	1:100/1:1000	IF/WB
mouse anti-Troponin I	(3)	1:200	IF
mouse anti-β-tubulin	Sigma	1:1000	WB
mouse anti ubiquitin	Enzo Life Sciences	1:100/1:1000	IP/WB

Supplementary Table 5. Primary antibodies used in this study.

1. Colombatti, A., Bonaldo, P., and Bucciotti, F. 1992. Stable expression of chicken type-VI collagen alpha 1, alpha 2 and alpha 3 cDNAs in murine NIH/3T3 cells. *Eur J Biochem* 209:785-792.
2. Wessels, A., Vermeulen, J.L., Viragh, S., Kalman, F., Lamers, W.H., and Moorman, A.F. 1991. Spatial distribution of "tissue-specific" antigens in the developing human heart and skeletal muscle. II. An immunohistochemical analysis of myosin heavy chain isoform expression patterns in the embryonic heart. *Anat Rec* 229:355-368.
3. Saggin, L., Gorza, L., Ausoni, S., and Schiaffino, S. 1989. Troponin I switching in the developing heart. *J Biol Chem* 264:16299-16302.

Gene	Forward Primer (5'-3')	Reverse Primer (5'-3')
Atrogin1/MAFbx	GCA AACACTGCCACATTCTCTC	CTTGAGGGGAAAGTGAGACG
ATF4	TCCTGAACAGCGAAGTGTTG	ACCCATGAGGTTTCAAGTGC
CHOP	GCTGGAAGCCTGGTATGAG	ATGTGCGTGTGACCTCTGTT
GADD34	AGAGAAGACCAAGGGACGTG	CAGCAAGGAATGGACTGTG
GAPDH	CACCATCTTCCAGGAGCGAG	CCTTCTCCATGGTGGTGAAGAC

Supplementary Table 6. Primers used in RTqPCR analyses.